Key Points:
- Short-term variability in thermospheric NO is consistently evaluated between SOFIE and SNOE observations
- NO high-latitude variability is dominated by geomagnetic variability, whereas low-latitude variability is driven by irradiance changes
- Response to a given geomagnetic forcing does not appear to vary with the phase of the solar cycle

Correspondence to:
K. Hendrickx,
koen.hendrickx@misu.su.se

Relative Importance of Nitric Oxide Physical Drivers in the Lower Thermosphere

Koen Hendrickx[1] [ID], **Linda Megner[1], Daniel R. Marsh[2]** [ID], **Jörg Gumbel[1], Rickard Strandberg[3],** and **Felix Martinsson[3]**

[1]Department of Meteorology, Stockholm University, Stockholm, Sweden, [2]National Center for Atmospheric Research, Boulder, CO, USA, [3]Department of Mathematics, Stockholm University, Stockholm, Sweden

Abstract Nitric oxide (NO) observations from the Solar Occultation for Ice Experiment and Student Nitric Oxide Explorer satellite instruments are investigated to determine the relative importance of drivers of short-term NO variability. We study the variations of deseasonalized NO anomalies by removing a climatology, which explains between approximately 70% and 90% of the total NO budget, and relate them to variability in geomagnetic activity and solar radiation. Throughout the lower thermosphere geomagnetic activity is the dominant process at high latitudes, while in the equatorial region solar radiation is the primary source of short-term NO changes. Consistent results are obtained on estimated geomagnetic and radiation contributions of NO variations in the two data sets, which are nearly a decade apart in time. The analysis presented here can be applied to model simulations of NO to investigate the accuracy of the parametrized physical drivers.

1. Introduction

NO has since long been recognized to be one of the important species of the lower thermosphere to efficiently radiate energy to space (Kockarts, 1980) and to change the composition of the ionosphere due to its low ionization threshold (Barth, 1995). The detailed NO chemistry has been described in several publications (Bailey et al., 2002; Barth, 1992; Roble, 1995) and is driven by solar irradiance and geomagnetic activity. Production of NO occurs primarily through the reaction of molecular oxygen with ground state and excited nitrogen atoms, which are created by ionization and dissociation of N_2 via solar soft X-rays and subsequent photoelectrons, extreme ultraviolet (EUV), and via precipitating auroral electrons (Barth et al., 1999; Gérard et al., 1995; Siskind et al., 1990; Siskind, Barth, Evans et al., 1989; Siskind, Barth, & Roble, 1989). NO loss occurs via interaction with ground state nitrogen or ionized molecular oxygen and via photodissociation by solar far ultraviolet (FUV) radiation below 190.8 nm (Barth, 1995), resulting in a long lifetime of NO in the dark, polar winter.

In this work we perform a series of multiple linear regressions (MLR) to investigate the drivers of NO variability in two satellite data sets taken approximately a decade apart. The MLR approach has been used before by Mlynczak et al. (2015) to study the long-term effects and relative importance of geomagnetic activity and solar radiation to global radiative NO cooling. Mlynczak et al. (2015) found that on average a 70% contribution of solar UV radiation and a 30% contribution due to geomagnetic processes determines the NO radiative cooling in the global lower thermosphere (100–250 km), with a strong solar cycle variability. We will demonstrate different results when assessing the short-term NO number density variability in specific latitudinal regions. A similar MLR approach to create an NO transfer function for comparing data sets of several satellites was used by Bender et al. (2015). They performed this regression with latitude as an additional component. Bender et al. (2015) note that differences in instrument sampling patterns remain and can introduce a bias in the analysis. Different satellites have different sampling patterns, hence different biases. In section 2 we describe our regression method that takes these biases into account as much as possible.

2. Data and Methodology

Observations from the Solar Occultation for Ice Experiment (SOFIE) instrument on board the Aeronomy of Ice in the Mesosphere (AIM) satellite (Gordley et al., 2009) are available from May 2007 (sofie.gats-inc.com) and have been previously described by Gómez-Ramírez et al. (2013) and Hendrickx et al. (2015). In this work the NO density version 1.3 is used from the start of observations until January 2015: a period that covers the
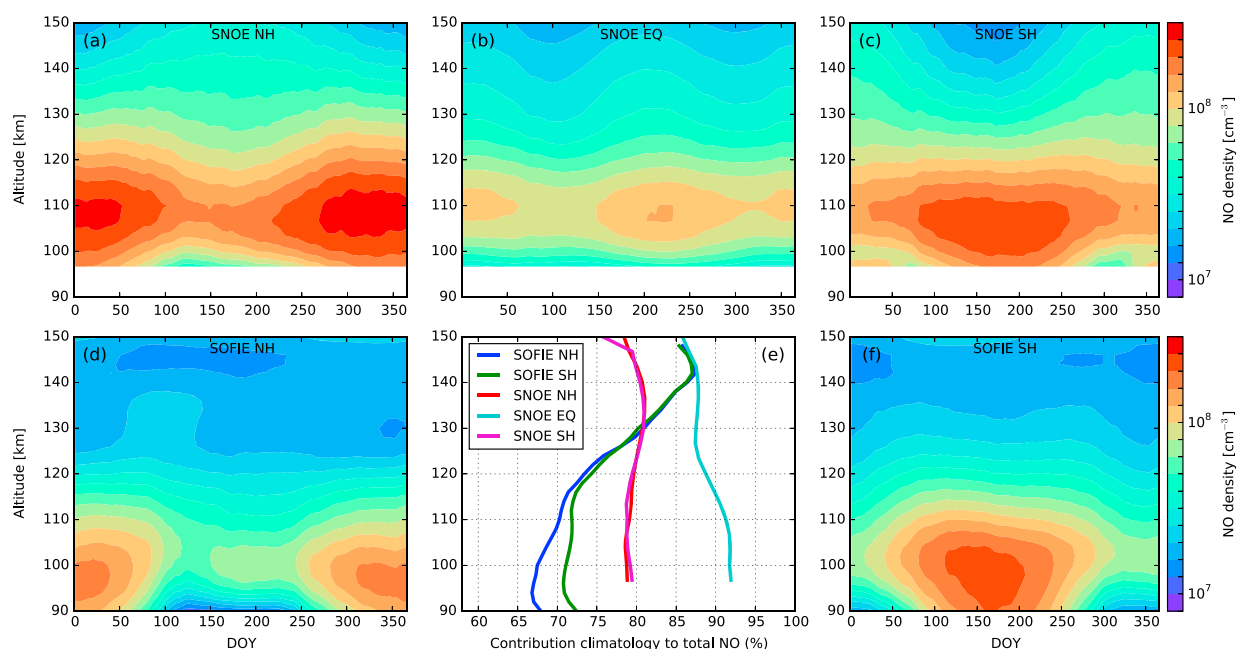
Figure 1. Multiyear mean climatology of (a–c) SNOE and (d, f) SOFIE NO observations in the lower thermosphere in function of day of year. SNOE data are averaged by latitude between 55° and 82.5° north and south and between ±15° around the equator. (e) The average percentage contribution of the climatological value to the total NO budget.

deep solar minimum between solar cycles (SC) 23 and 24, and the ascending and maximum phase of SC 24. The observations are focused on high latitudes ranging between 55° and 82.5° latitude with local sunset/sunrise measurements in the Northern/Southern Hemisphere (NH/SH), respectively, and are sampled on one latitude at a given time of year. A zonally and meridionally averaged climatology of NO in the lower thermosphere is shown in Figures 1d and 1f for each hemisphere. The thermospheric NO maximizes between 95 and 105 km altitude and peaks in density during winter, representing a lower limit of NO in the dark polar regions due to the solar occultation technique.

We also use Student Nitric Oxide Explorer (SNOE) observations (Solomon et al., 1996) to complement and confirm our results. The SNOE satellite determined NO densities with an ultraviolet spectrometer and provided data from 11 March 1998 to 30 September 2000 (ascending phase of SC 23) so observations are almost a decade apart from the SOFIE era. Obtaining consistent results between both data sets is therefore a strong indication of real physical processes. SNOE observations have been intensively studied (e.g., Barth & Bailey, 2004; Marsh et al., 2004; Solomon et al., 1999), and in this work SNOE level 4 data (lasp.colorado.edu/home/snoe/) are averaged by latitude from 55° poleward for high latitudes and between ±15° around the equator. SNOE climatologies are shown in Figures 1a–1c and show a different seasonal cycle from SOFIE observations.

NO variation in the lower thermosphere is represented by short-term geomagnetic activity, solar radiation, and seasonality. We choose the auroral electrojet (*AE*) index as proxy for geomagnetic activity as it focuses on the polar regions and correlates better with NO concentrations in SOFIE observations than the planetary *Ap* index (Hendrickx et al., 2015). The response in the NO peak density altitude layer, around 105 km, to geomagnetic activity is typically lagged by 1 day (Solomon et al., 1999; Hendrickx et al., 2015) but is dependent on altitude (Fytterer et al., 2016). Since we are interested in the NO response throughout the lower thermosphere, we use an *AE* value averaged over the past 2 days. As proxy for solar irradiance the Lyman-α (Lyα) index, a spectral line of solar hydrogen, is used. Lyman-α radiation does not play a direct role in NO production processes but is a proxy for soft X-rays, EUV, and FUV (Lean, 1987), which, as explained in the introduction, are the wavelengths of importance to the NO reactions. Alternative choices as proxies for solar irradiance include direct observations of solar soft X-rays or the $F_{10.7}$ solar radio flux, which is a common used proxy for soft X-rays. However, all these indices are highly correlated and the results were not significantly effected whether $F_{10.7}$ or solar soft X-rays were used instead. Seasonality could be represented by, for example, sinusoidal functions

(Bender et al., 2015) or solar declination (Marsh et al., 2004). However, the observed seasonality differs between the NO data sets and is limited to the subset of local times and latitudes at which each satellite samples, hence a representation for seasons would be different for different satellites. In order to be able to compare different satellites, we instead remove the climatology of each data set, in which seasons and biases are imbedded, and regress on variations. The climatology is calculated as a moving 90 day window of the multiyear mean of each date.

The executed regression follows

$$\Delta \text{NO}(z, AE, \text{Ly}\alpha, t) = \gamma_{AE}(z)\Delta AE(t) + \gamma_{\text{Ly}\alpha}(z)\Delta \text{Ly}\alpha(t) + \epsilon(z, t),\tag{1}$$

where γ_{AE} and $\gamma_{\text{Ly}\alpha}$ are the estimated coefficients of the corresponding AE and $\text{Ly}\alpha$ regressors and ϵ the residual error term. Here ΔNO (ΔAE, $\Delta \text{Ly}\alpha$) denotes the anomaly of NO (AE, $\text{Ly}\alpha$) from its climatological value. All variables in the MLR are scaled to have zero mean and unit variance. The regression is performed for different altitudes z with a vertical sampling of 2 km on SOFIE data and 3.3 km for SNOE data. Autocorrelation in the residual ϵ terms was tested with the Durbin-Watson test (Durbin & Watson, 1950) and found to be present. If not corrected for, autocorrelation can result into an overestimated R^2 value of the regression model and biased estimated regressor coefficients. The Cochrane-Orcutt procedure (Cochrane & Orcutt, 1949) was applied on the NO data ensuring unbiased results and minimized residual autocorrelation.

The total coefficient of determination R_{tot}^2 of the MLR model can be defined as

$$\begin{aligned} R_{\text{tot}}^2 &= R_{\text{model}}^2 + R_{\text{auto}}^2 \\ &= 1 - R_{\text{res}}^2, \end{aligned}\tag{2}$$

with R_{model}^2, R_{auto}^2, and R_{res}^2 being the variation explained by the model, autocorrelation, and residuals, respectively. Each R^2 value is given by the sums of squares ratio

$$\begin{aligned} R_{\text{model}}^2 &= \frac{\text{SS}_{\text{model}}}{\text{SS}_{\text{tot}}} = \frac{\sum_i (\hat{y}_i - \bar{y})^2}{\sum_i (y_i - \bar{y})^2}, \\ R_{\text{res}}^2 &= \frac{\text{SS}_{\text{res}}}{\text{SS}_{\text{tot}}} = \frac{\sum_i (y_i - \hat{y}_i)^2}{\sum_i (y_i - \bar{y})^2}, \\ R_{\text{auto}}^2 &= \frac{\text{SS}_{\text{tot}} - \text{SS}_{\text{model}} - \text{SS}_{\text{res}}}{\text{SS}_{\text{tot}}}, \end{aligned}\tag{3}$$

with y_i and $\hat{y}_i$ the observational and modeled values and $\bar{y}$ the observational mean. The R_{model}^2 can be further subdivided into $R_{\text{model}}^2 \approx R_{AE}^2 + R_{\text{Ly}\alpha}^2$ to reveal the contribution of geomagnetic activity and solar radiation to the NO variability and where intercorrelation effects between ΔAE and $\Delta \text{Ly}\alpha$ are small ($r < 0.10$ during SNOE observations and $r < 0.28$ during SOFIE observations).

The interpretation of the analysis is such that NO densities are largely predictable by the climatological value, which exhibits a seasonal component, and that physical drivers cause a deflection (positive or negative) of this climatology. The percentage contribution of the climatology to the total NO budget is given in Figure 1e and shows that it ranges from approximately 70% at the polar latitudes where auroral electrons precipitate, to 90% at the equator. The magnitude of γ_{AE} and $\gamma_{\text{Ly}\alpha}$ indicate which driver is dominant and the corresponding R_{AE}^2 and $R_{\text{Ly}\alpha}^2$ give the percentage contribution. The R_{tot}^2 of the model gives an indication on how much of the short-term NO variation can be explained by the two drivers and by autocorrelation, and on how large the unexplained residual variation is.

3. Results

The AE and $\text{Ly}\alpha$ indices are shown in Figure 2 for both the SNOE and SOFIE observational time periods, spaced a decade apart in time. To indicate how solar cycles 23 and 24 progressed, the evolution of the indices around and between the satellite periods is given. The activity in terms of solar radiation is stronger in the ascending phase of SC 23 with a continuous increase from 1998 to 2001, followed by fairly flat Lyman-α activity in the deep solar minimum of 2008–2010 and a slow, gradual increase toward solar maximum in 2013–2014. With respect to the geomagnetic driver, periods of high and low activity can be found in both solar cycles and a strong 27 day periodicity is present. Differences in proxy activity between SC 23 and SC 24 are thus
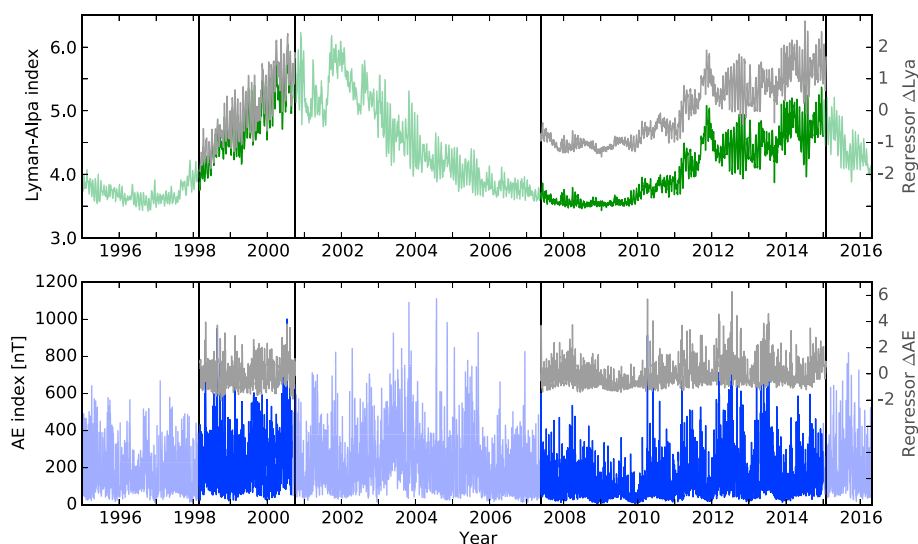
Figure 2. Time evolution of the (top) Lyman-α and (bottom) AE indices during SC 23 and 24. The observational period of SNOE and SOFIE are highlighted between black lines. Green and blue lines represent the absolute index value of Lyman-α and AE in units 10^{11} photons cm^{-2} s^{-1} and nT, respectively. Gray lines are the scaled, unitless regressors that serve as input to the MLR (see section 2 for details).

present and can have an influence on the estimated γ coefficients. However, by scaling the regressors to unit variance and zero mean, the MLR-fitted coefficients are directly comparable in terms of strength and the relative importance of each regressor can be determined. The regressors ΔAE and $\Delta Ly\alpha$ are shown in gray lines in Figure 2 and serve as input to the MLR.

Figure 3 shows the result of the MLR for both SOFIE and SNOE data in four panels; the explained variation for each regression model is given in Figures 3a and 3b for SOFIE and SNOE, respectively, while the estimated coefficients γ_{AE} and $\gamma_{Ly\alpha}$ are given in Figures 3c and 3d, respectively. To test the influence of latitude, we performed regressions at high latitudes (averaged between 55° and 82.5°) on both data sets and at equatorial latitudes ($\pm 15°$) on SNOE data. The total explained variance for the SNOE high latitudes indicates that up to 80% of the observed NO anomalies is given by the two regressors, the rest is due to residual variation. R^2_{tot} decreases with increasing altitude as NO densities decrease and the signal-to-noise ratio of the observation increases. A similar result is obtained for SOFIE data with the total explained variation dropping below 50% at 126 (132) km for NH (SH) data, which implies that above these altitudes more than 50% is due to residual variation. This residual variation can be a result of random processes such as instrumental noise and may also contain processes that are known to affect NO densities, such as Joule heating and compressional heating (Barth, 1995), which are not represented by the two proxies used. When the R^2_{tot} value becomes this low, the regression is not sufficient to draw physical meaning from the output; we therefore neglect any output if $R^2_{\text{tot}} < 0.5$.

Below 110 km autocorrelation becomes more important, a feature seen in both data sets. This implies that NO anomalies at these altitudes are less determined by the AE and Lyα variations and are increasingly more dependent on previous day values, which is to be expected as downward transport becomes a major source of NO at these altitudes.

The estimated coefficient γ_{AE} for geomagnetic activity is given in Figure 3c. At high latitudes both data sets show that the effect of precipitating particles on NO is largest above 110 km altitude. SOFIE observes an overall higher impact of EPP in the SH while for SNOE the impact is similar in both hemispheres. At altitudes below 110 km the impact of EPP on NO variations decreases as fewer energetic particles reach these altitudes. Below 100 km, downward transport also becomes prominent and the NO anomalies are therefore increasingly governed by previous day NO values. Dependent on altitude, geomagnetic activity contributes between 5% and 70% to the NO variability at high latitudes, with the maximum contribution between 110 and 120 km.

The estimated coefficient $\gamma_{Ly\alpha}$ for solar radiation is shown Figure 3d and can be directly compared to γ_{AE} since both regressors are scaled. Throughout the lower thermosphere the impact of radiation on NO variations
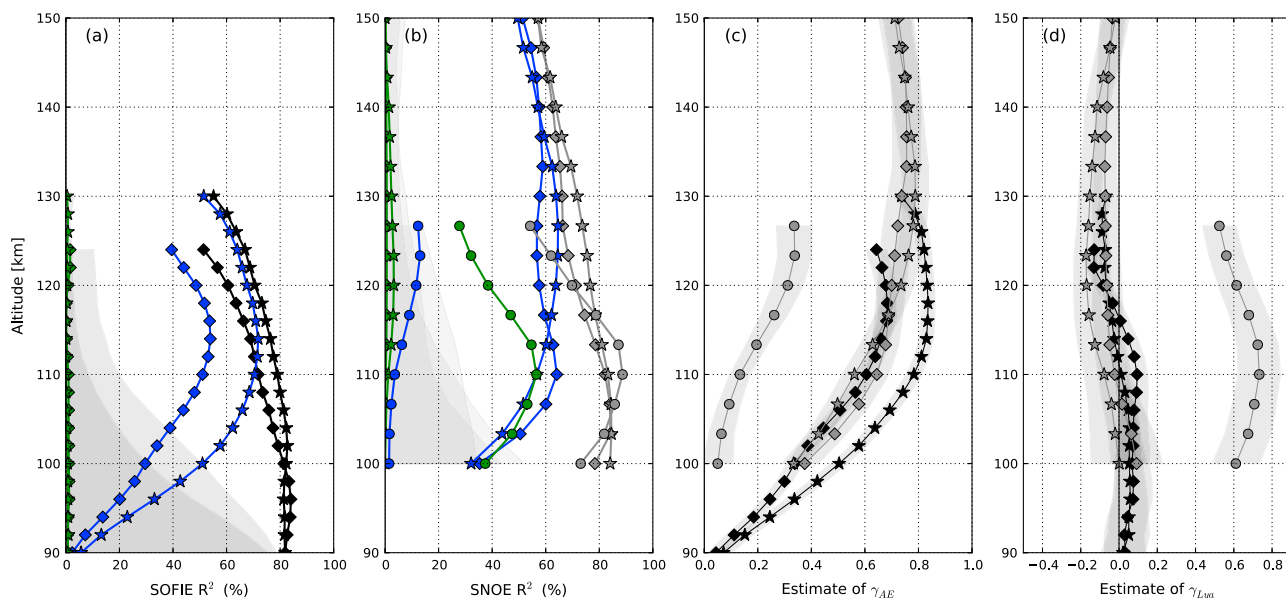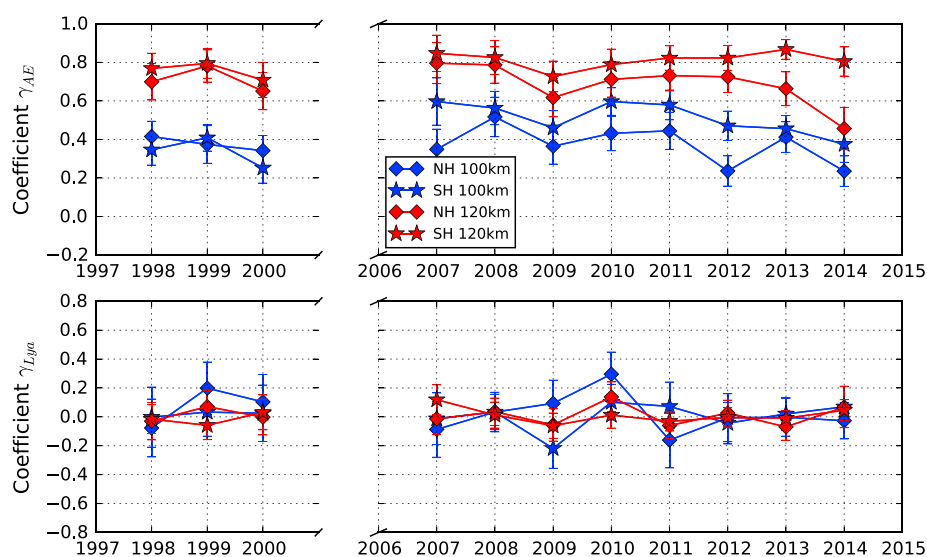
Figure 3. Results of the MLR performed on SOFIE (black) and SNOE (gray) data, in the NH (diamonds), SH (stars), and equatorial region (circles) throughout the lower thermosphere. (a) SOFIE data. Total explained variation as represented by R^2_{tot} (see equation (1), which is the sum of R^2_{AE} (blue), $R^2_{Ly\alpha}$ (green), and R^2_{auto} (shaded area). The unexplained residual variation equals $1 - R^2_{tot}$. (b) Similar as Figure 3a for SNOE data. (c) Estimates for the coefficients of geomagnetic activity. (d) Estimates for the coefficients of solar radiation. The estimated coefficients can directly be compared to each other.

is significantly smaller ($< 4\%$) than the geomagnetic impact at high latitudes, similar to Barth et al. (2003). For SNOE data, the coefficient is slightly negative implying that the net effect of radiation is a destruction of NO and that the destructive processes connected to solar radiation are stronger than the production processes at these high latitudes. A similar result was obtained when using the co-observed solar soft X-rays from the SNOE satellite instead of the Lyman-α index as regressor. However, we cannot exclude that this small negative impact is an artifact of the MLR algorithm, for instance, connected to the long-term relation between the regressors. As will be discussed in the last paragraph of this section, the impact is generally consistent with zero for any independent year.

To contrast the NO drivers at high latitudes, we also performed regressions at the equatorial regions on SNOE data. The impact of solar radiation is clearly higher than the geomagnetic activity impact and as can be seen from the positive $\gamma_{Ly\alpha}$ coefficient, solar radiation is a source of NO in the equatorial lower thermosphere. Similar to Barth et al. (2003), the irradiance impact in equatorial regions maximizes around 113 km, implying vertical mixing from that altitude toward 106 km, the altitude of maximum NO concentrations as observed by SNOE. A small impact of geomagnetic activity ($<15\%$) contributes to the NO variations and peaks at higher altitudes than the impact at high latitudes. This can be due to precipitating electrons from the equatorial ring currents, Joule, and subsequent compressional heating in the high to middle latitudes or horizontal transport, or a combination of these processes (Barth, 1995; Barth et al., 2009; Richards, 2004).

Solar activity varies with an approximately 11 year periodicity, but corresponding phases of different cycles can differ substantially in intensity or be shifted in time. For instance, the solar minimum between SC 23 and 24 in 2008 and 2009 was of particularly long duration and the ascending phase of SC 24 saw a more gradual increase in Lyman-α activity compared to the previous cycle (see Figure 2). In order to investigate whether long-term solar activity impacts the regression coefficients, we perform regressions for each year and show the results at an altitude of 100 and 120 km in Figure 4. A higher AE coefficient in 1 year would indicate that NO anomalies were more sensitive to geomagnetic activity, but the retrieved γ_{AE} for each year is rather stable, and the small variation is within the statistical noise level. Moreover, the estimated geomagnetic impact during SC 23 shows similar sensitivity and is consistent with the impact during SC 24, again indicating that these coefficients are rather constant throughout the solar cycle. The yearly impact of solar radiation becomes consistent with zero as variations in Lyα during 1 year are limited and only short-term variations are considered.

Figure 4. Results of the MLR performed at 100 km (blue) and 120 km (red) altitude on yearly SNOE (1998–2000) and SOFIE (2007–2014) data, in the NH (diamonds) and SH (stars) high latitudes. Estimated coefficients with a 2σ error bar are shown for (top row) geomagnetic activity γ_{AE} and (bottom row) solar radiation $\gamma_{Ly\alpha}$.

4. Discussion and Conclusions

The relative importance of the main drivers of NO variability in the lower thermosphere, geomagnetic activity, and solar radiation is investigated in this study. New observations from the SOFIE instrument are analyzed and complemented with data from the SNOE satellite, covering more latitude regions and a different time span. NO climatologies of both data sets show that long-term averages contribute between 70% and 90% to the total observed NO number density, depending on altitude and latitude. To determine the short-term impact of the drivers and compare different satellite data sets, we applied a series of multiple linear regressions on data of which the climatology is removed and that has been scaled to unit variance and mean zero. By removing the climatology, we remove as much intrinsic differences as possible in each NO data set such as observation techniques or latitudinal sampling and remain with the short-term variation which we want to describe in terms of physical processes. This allows us to compare observations from different satellites. Scaling the regressors allows us to study the relative importance of the drivers percentage.

The two data sets, spaced a decade apart in time, gave consistent results when comparing similar latitude bands: at high latitudes geomagnetic activity accounts up to 70% of the NO variability, while the contribution of solar radiation is small to negligible. NO anomalies become increasingly more autocorrelated at decreasing altitudes below 110 km, which implies a smaller impact from the physical drivers. At equatorial regions it is solar radiation that dominates variability in NO and its impact can be up to 8 times larger than geomagnetic effects. The estimated regression coefficients γ_{AE} and $\gamma_{Ly\alpha}$ do not describe how much total NO is produced by AE and Lyα but rather show how much the variability of AE and Lyα impacts the NO production, and their magnitude is a measure of their relative importance. SOFIE observations reveal a larger geomagnetic impact in the SH than in the NH, while SNOE observations show no difference. Since the local time of observation of SOFIE coincides with sunrise/sunset in the SH/NH, this could be a possible explanation for the different geomagnetic impact: the signature of geomagnetic activity remains in NO densities throughout the SH night (even when removing the SH climatology), while sunlight in the NH could have already partly destroyed that signature.

Finally, we show that there is no significant year to year variation of the regression coefficients at high latitudes, implying that they are not sensitive to the phase of the 11 year solar cycle. The fact that the coefficients remain stable with respect to the solar cycle means that even though geomagnetic activity and solar radiation change, the impact on NO due to a certain increase/decrease in these quantities remains the same. It implies that once we know how much NO changes due to a certain AE change in one part of the solar cycle, we can directly apply this knowledge to calculate the expected change in another part of the solar cycle.

Further, the consistency of the results indicates that the method is robust in identifying key processes in NO density variations and that it can be used as a diagnostic tool in model simulations to evaluate the accuracy of the parametrizations of NO production.

References

Bailey, S. M., Barth, C. A., & Solomon, S. C. (2002). A model of nitric oxide in the lower thermosphere. *Journal of Geophysical Research*, *107*(A8), SIA 22–SIA 21. https://doi.org/10.1029/2001JA000258

Barth, C. A. (1992). Nitric oxide in the lower thermosphere. *Planetary and Space Science*, *40*(2–3), 315–336. https://doi.org/10.1016/0032-0633(92)90067-X

Barth, C. A. (1995). Nitric oxide in the lower thermosphere. In R. M. Johnson & T. L. Killeen (Eds.), *The Upper Mesosphere and Lower Thermosphere: A Review of Experiment and Theory, Geophysical Monograph Series* (Vol. 87, pp. 225–233). Washington, DC: American Geophysical Union. https://doi.org/10.1029/GM087p0225

Barth, C. A., & Bailey, S. M. (2004). Comparison of a thermospheric photochemical model with Student Nitric Oxide Explorer (SNOE) observations of nitric oxide. *Journal of Geophysical Research*, *109*, A03304. https://doi.org/10.1029/2003JA010227

Barth, C. A., Bailey, S. M., & Solomon, S. C. (1999). Solar-terrestrial coupling: Solar soft X-rays and thermospheric nitric oxide. *Geophysical Research Letters*, *26*(9), 1251–1254. https://doi.org/10.1029/1999GL900237

Barth, C. A., Lu, G., & Roble, R. G. (2009). Joule heating and nitric oxide in the thermosphere. *Journal of Geophysical Research*, *114*, A05301. https://doi.org/10.1029/2008JA013765

Barth, C. A., Mankoff, K. D., Bailey, S. M., & Solomon, S. C. (2003). Global observations of nitric oxide in the thermosphere. *Journal of Geophysical Research*, *108*, 1027. https://doi.org/10.1029/2002JA009458

Bender, S., Sinnhuber, M., von Clarmann, T., Stiller, G., Funke, B., López-Puertas, M., ... Burrows, J. (2015). Comparison of nitric oxide measurements in the mesosphere and lower thermosphere from ACE-FTS, MIPAS, SCIAMACHY, and SMR. *Atmospheric Measurement Techniques*, *8*(10), 4171–4195. https://doi.org/10.5194/amt-8-4171-2015

Cochrane, D., & Orcutt, G. H. (1949). Application of least squares regression to relationships containing auto-correlated error terms. *Journal of the American Statistical Association*, *44*(245), 32–61. https://doi.org/10.1080/01621459.1949.10483290

Durbin, J., & Watson, G. S. (1950). Testing for serial correlation in least squares regression. I. *Biometrika*, *37*(3–4), 409. https://doi.org/10.1093/biomet/37.3-4.409

Fytterer, T., Bender, S., Berger, U., Nieder, H., Sinnhuber, M., & Wissing, J. (2016). Model studies of short-term variations induced in trace gases by particle precipitation in the mesosphere and lower thermosphere. *Journal of Geophysical Research: Space Physics*, *121*, 10,431–10,447. https://doi.org/10.1002/2015JA022291

Gérard, J.-C., Shematovich, V. I., & Bisikalo, D. V. (1995). The role of fast N(^{4}s) atoms and energetic photoelectrons on the distribution of NO in the thermosphere. In R. M. Johnson & T. L. Killeen (Eds.), *The Upper Mesosphere and Lower Thermosphere: A Review of Experiment and Theory Geophysical Monograph Series* (Vol. 87, pp. 235–241). Washington, DC: American Geophysical Union. https://doi.org/10.1029/GM087p0225

Gómez-Ramírez, D., McNabb, W. C., Russel, J. M., Hervig, M. E., Deaver, L. E., Paxton, G., & Bernath, P. F. (2013). Empirical correction of thermal responses in the solar occultation for ice experiment nitric oxide measurements and initial data validation results. *Applied Optics*, *52*(13), 2950–2959. https://doi.org/10.1364/ao.52.002950

Gordley, L. L., Hervig, M. E., Fish, C., Russell III, J. M., Bailey, S., Cook, J., ... Kemp, J. (2009). The solar occultation for ice experiment. *Journal of Atmospheric and Solar-Terrestrial*, *71*, 300–315. https://doi.org/10.1016/j.jastp.2008.07.012

Hendrickx, K., Megner, L., Gumbel, J., Siskind, D. E., Orsolini, Y. J., Tyssøy, N. H., & Hervig, M. (2015). Observation of 27 day solar cycles in the production and mesospheric descent of EPP-produced NO. *Journal of Geophysical Research: Space Physics*, *120*, 8978–8988. https://doi.org/10.1002/2015JA021441

Kockarts, G. (1980). Nitric oxide cooling in the terrestrial thermosphere. *Geophysical Research Letters*, *7*(2), 137–140. https://doi.org/10.1029/GL007i002p00137

Lean, J. (1987). Solar ultraviolet irradiance variations: A review. *Journal of Geophysical Research*, *92*(D1), 839–868. https://doi.org/10.1029/JD092id01p00839

Marsh, D. R., Solomon, S. C., & Reynolds, A. E. (2004). Empirical model of nitric oxide in the lower thermosphere. *Journal of Geophysical Research*, *109*, A07301. https://doi.org/10.1029/2003JA010199

Mlynczak, M. G., Hunt, L. A., Marshall, T. B., Russell, J. M., Mertens, C. J., Thompson, E. R., & Gordley, L. L. (2015). A combined solar and geomagnetic index for thermospheric climate. *Geophysical Research Letters*, *42*, 3677–3682. https://doi.org/10.1002/2015GL064038

Richards, P. (2004). On the increases in nitric oxide density at midlatitudes during ionospheric storms. *Journal of Geophysical Research*, *109*(A6), A06304. https://doi.org/10.1029/2003JA010110

Roble, R. G. (1995). Energetics of the mesosphere and thermosphere. In R. M. Johnson & T. L. Killeen (Eds.), *The Upper Mesosphere and Lower Thermosphere: A review of Experiment and Theory Geophysical Monograph Series* (Vol. 87, pp. 1–21). Washington, DC: American Geophysical Union. https://doi.org/10.1029/GM087p0001

Siskind, D. E., Barth, C. A., & Cleary, D. (1990). The possible effect of solar soft X-rays on thermospheric nitric oxide. *Journal of Geophysical Research*, *95*(A4), 4311–4317. https://doi.org/10.1029/JA095ia04p04311

Siskind, D. E., Barth, C. A., Evans, D. S., & Roble, R. G. (1989). The response of thermospheric nitric oxide to an auroral storm: 2. Auroral latitudes. *Journal of Geophysical Research*, *94*(A12), 16,899–16,911. https://doi.org/10.1029/JA094iA12p16899

Siskind, D. E., Barth, C. A., & Roble, R. G. (1989). The response of thermospheric nitric oxide to an auroral storm: 1. Low and middle latitudes. *Journal of Geophysical Research*, *94*(A12), 16,885–16,898. https://doi.org/10.1029/JA094ia12p16885

Solomon, S. C., Barth, C. A., Axelrad, P., Bailey, S. M., Brown, R., Davis, R. L., ... Woods, T. N. (1996). The student nitric oxide explorer. *Proceedings of the SPIE: Space Sciencecraft Control and Tracking in the New Millennium*, *2810*, 121–132. https://doi.org/10.1117/12.255131

Solomon, S. C., Barth, C. A., & Bailey, S. M. (1999). Auroral production of nitric oxide measured by the SNOE satellite. *Geophysical Research Letters*, *26*(9), 1259–1262. https://doi.org/10.1029/1999GL900235